Desalination and Water Treatment
www.deswater.com

doi: 10.5004/dwt.2020.25390

185 (2020) 307–317
May

Converting *Hylocereus undatus* (white dragon fruit) peel waste into a useful potential adsorbent for the removal of toxic Congo red dye

Linda B.L. Lim[a,*], Namal Priyantha[b,c], Siti Amanina Abdul Latip[a], Yie Chen Lu[a], Abdul Hanif Mahadi[d]

[a]*Department of Chemistry, Faculty of Science, Universiti Brunei Darussalam, Jalan Tungku Link, Gadong, Negara Brunei Darussalam, Tel. 00-673-8748010; emails: linda.lim@ubd.edu.bn (L.B.L. Lim), nyna.al611@gmail.com (S.A.A. Latip), yiechen_93@hotmail.com (Y.C. Lu)*
[b]*Department of Chemistry, Faculty of Science; University of Peradeniya, Peradeniya, Sri Lanka, namal.priyantha@yahoo.com (N. Priyantha)*
[c]*Postgraduate Institute of Science, University of Peradeniya, Peradeniya, Sri Lanka*
[d]*Centre for Advanced Material and Energy Sciences, Universiti Brunei Darussalam, Jalan Tungku Link, Gadong, Negara Brunei Darussalam, email: hanif.mahadi@ubd.edu.bn (A.H. Mahadi)*

Received 15 August 2019; Accepted 22 December 2019

A B S T R A C T

Dragon fruits are considered as exotic fruits and have recently gained popularity due to their health benefits in having high nutritional values and good antioxidant properties. The peels, being inedible, are discarded as wastes. In this study, white dragon fruit peel (WDFP) was utilized as a potential low-cost natural adsorbent for the removal of toxic Congo red (CR) dye. This is the first report on the use of WDFP as an adsorbent. Previous reports on white dragon fruit were based on utilizing its foliage. The WDFP-CR system achieved equilibrium within 3 h. WDFP, whose point of zero charges was determined to be at pH 5.02, exhibits good overall resilience to changes in both pH medium and ionic strength. Adsorption isotherm indicated the Temkin model to be the best fit followed by the Sips model with high maximum adsorption capacity (q_{max}) of 76.6 mg g^{-1} as compared to many other reported natural adsorbents. Adsorption process using 100 mg L^{-1} CR dye confirmed the pseudo-second-order kinetics with rate constant k_2 of 1.87 g mmol^{-1} min^{-1}. The Weber and Morris model indicated that intraparticle diffusion of CR into WDFP could be the rate-determining step. WDFP can be regenerated and was found to be reusable up to 4 consecutive cycles when using acid as the desorbing solvent.

Keywords: Hylocereus undatus; Dragon fruit waste; Adsorption isotherm; Congo red; Azo dye; Kinetics

1. Introduction

Combating environment pollution is a matter of urgency for if left unattended, it will result in adverse effects on human health and the quality of life. Of the various types of environmental pollution, wastewater pollution has received much attention since all life forms depend on water for survival. Even though there is approximately 70% water on Earth, yet of these only, less than 3% is made up of fresh water. Over the past couple of decades with the industrial boom and rapid rise in the world's population, dumping of wastes have resulted in severe wastewater pollution. For example, toxic synthetic dyes and their corresponding waste by-products not only are dangerous when consumed, but they also result in intense colors in rivers and streams giving rise to detrimental effects on aquatic life. Their persistent stability and colors prevent sunlight from penetrating, thereby

* Corresponding author.

1944-3994/1944-3986

reduce photosynthesis of algae. As a consequence, this disrupts the food chain and the eco-system.

Various methods have been employed over the years in an attempt to treat wastewater [1–3]. Adsorption using low-cost adsorbents has proved to be one of the most successful methods in wastewater treatment [4]. The method is simple, easy, straightforward and at the same time effective and low cost. Various adsorbents have been tested and they range from agro wastes [5–7] to industrial wastes [8], synthetic materials [9], modified adsorbents [10–12] and many others [13–16].

Pitaya, or commonly known as dragon fruits, have gained popularity over the years, not only as exotic fruits but also for their health benefits. Originally from tropical and subtropical America, dragon fruits belong to the Cactaceae family. Of the various varieties of pitaya, the two most popular being sold in Brunei Darussalam are the red (*Hylocereus polyrhizus*) and white (*Hylocereus undatus*) species, the latter being sold at a much cheaper price. The presence of phenolic compounds, betacyanins, betalains, and others suggests that dragon fruit peel could be utilized as a potential adsorbent with functional groups such as OH, C=O, C=C, NH, aiding in adsorption of adsorbates [17–20]. Further, both the red and white dragon fruit peel (WDFP) has been reported to be cytotoxic against PC3, Bcap-37, and MGC-803 cells [21].

To date, there have been some reports on the use of red dragon fruit (*Hylocereus polyrhizus*) peel as an adsorbent for the removal of dyes and heavy metals [22–26]. Surprisingly, the use of white dragon fruit (*Hylocereus undatus*) is scarce. Only two studies on the use of its foliage as an adsorbent to remove methylene blue [27] and methyl orange dyes have recently been reported [28]. However, no report on the use of WDFP has been found. Hence, this will be the first study on the use of WDFP as an adsorbent.

In this study, WDFP will be investigated for its adsorption characteristics toward Congo red (CR), whose structure is shown in Fig. 1. Discovered by Paul Bottinger in 1883, CR is the first direct dye to dye cotton without the use of a mordant [29]. It is an example of an azo dye and being brilliant red in color, the dye is used in the textile industry but is highly toxic and has carcinogenic effects [30,31]. One of the uses of CR is in histologic staining and is the dye of choice for diagnosis of amyloidosis [32]. A recent study showed that CR exhibits phytotoxicity to *Zea mays* and *Solanum lycopersicum* by retarding their germination [33]. Intravenous injection of CR has resulted in severe collapse and fatal death in patients [34].

2. Methods

2.1. Sample preparation

White dragon fruits (*Hylocereus undatus*) were randomly bought from the local supermarkets in the Brunei-Muara District of Negara Brunei Darussalam. The WDFP was separated from its edible flesh, dried at 60°C to a constant mass and the dried sample was grounded and sieved with laboratory metal sieve. WDFP with particle sizes <355 μm were collected and stored in sealed bags until ready to be used.

2.2. Selected adsorbate in this study

CR dye with molecular formula $C_{32}H_{22}N_6Na_2O_6S_2$ (Mr 696.66 g mol^{-1}) was selected as the model dye and was purchased from Sigma and used without further purification. The Shimadzu UV-1601 PC UV-visible spectrophotometer (Japan), set at wavelength 500 nm, was used to measure the absorbance of CR.

2.3. Optimization of parameters

Investigations into the time to reach equilibrium (0–4 h), pH effect (4–12) and effect of ionic strength using NaCl ranging from 0 to 1 mol dm^{-3} were carried out with WDFP (0.020 g) in 100 mg L^{-1} CR dye solution (10.0 mL). The WDFP-CR mixtures were shaken at 250 rpm at room temperature. Adjustment of pH was done using either 1.0 mol dm^{-3} HCl and/or NaOH.

2.4. Batch adsorption studies

All the batch adsorption studies carried out in this study were done by agitating a mixture of WDFP (0.020 g) in 10.0 mL of CR dye solution at 250 rpm, keeping the ratio of adsorbent: adsorbate to 1:500 (weight:volume) unless otherwise stated. Adsorption isotherm studies were carried out using CR dye concentrations ranging from 0 to

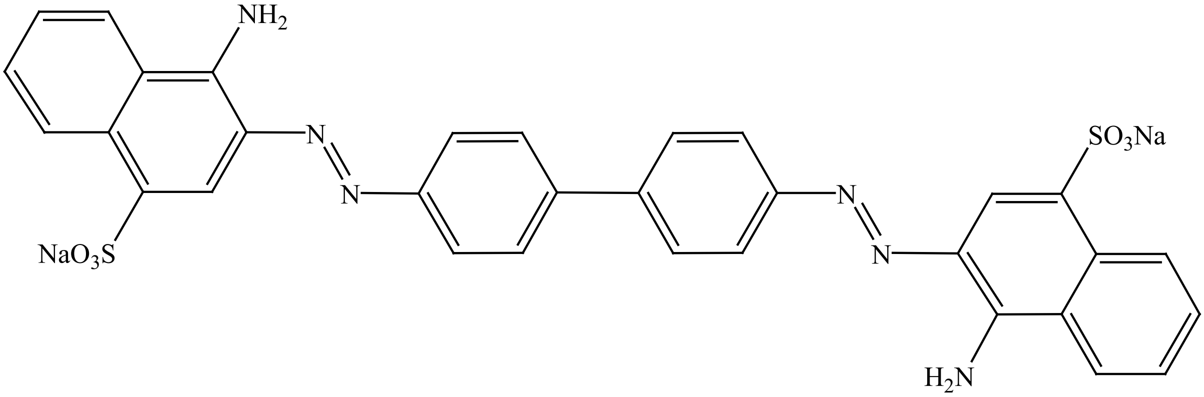

Fig. 1. Chemical structure of CR dye.

1,000 mg L^{-1}, whilst kinetics studies were investigated using 100 mg L^{-1} CR.

3. Results and discussion

3.1. Determination of the contact time required for adsorption of CR onto WDFP

The determination of the time required for an adsorbate–adsorbent system to attain equilibrium is one of the important parameters in adsorption studies. As shown in Fig. 2, adsorption of CR dye onto WDFP required 3 h for equilibrium to be reached. The rate of adsorption was fastest at the initial stage owing to the presence of empty vacant sites on the surface of the adsorbent, allowing CR dyes to be quickly adsorbed. As more of these sites were being filled, a decrease in the adsorption process was observed and gradually giving rise to a plateau indicating an equilibrium state was reached.

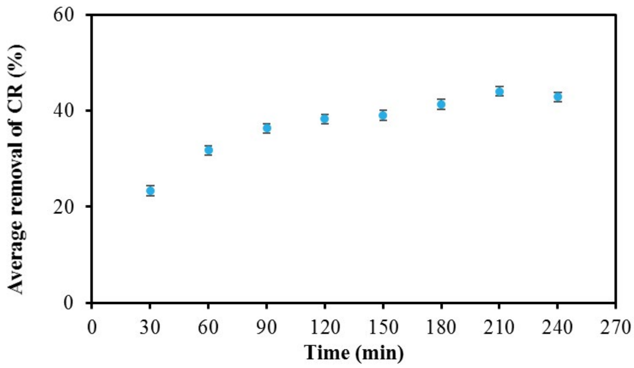

Fig. 2. Effect of contact time for the adsorption of CR by WDFP.

3.2. Effect of initial dye concentration on adsorption by WDFP

The effect of initial CR dye concentration was investigated and the results are depicted in Fig. 3. As the dye concentration increased from 0 to 1,000 mg L^{-1}, the amount of CR being adsorbed onto WDFP also increased. This behavior, in line with the Fick's laws of diffusion, is attributed to the increased driving force resulting from the increased concentration gradient which in turn helped to overcome the mass transfer resistance of CR between the WDFP-aqueous phases. On the other hand, the % removal of CR decreased with increasing dye concentration. This is due to the active binding sites on the surface of WDFP becoming more saturated at high concentrations. At low CR concentrations, the ratio of active sites to dye molecules is high, thus enabling more CR to be adsorbed onto the active sites of WDFP.

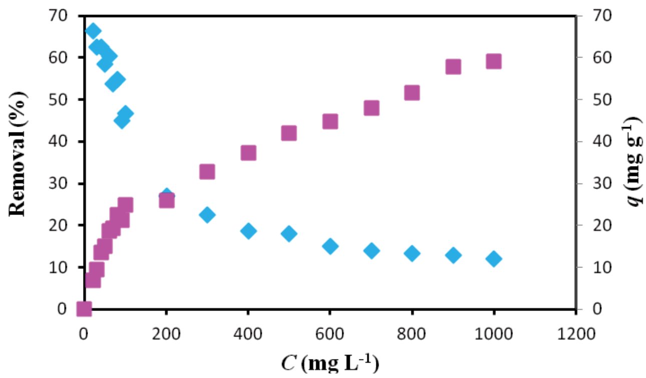

Fig. 3. Effect of dye concentration on the percentage removal (◆) and amount (■) of CR being adsorbed onto WDFP.

3.3. Adsorption isotherm of CR dye onto WDFP

Adsorption isotherm provides useful information of an adsorption process and in this study, five different isotherm models were employed to analyze the experimental data for the adsorption of CR onto WDFP, namely the Langmuir [35], Freundlich [36], Temkin [37], Redlich–Peterson (R–P) [38] and Sips [39] models. Five error functions, that is, average relative error (ARE), hybrid fractional error function (HYBRID), Marquardt's percent standard deviation (MSPD), sum of absolute error (EABS), non-linear chi-square test (χ^2), were also used to provide further accuracy on the selection of the best isotherm model, whereby the lower the error values, the more fitting the model will be. The non-linear equations of the isotherm models and equations of error functions are shown below in Table 1.

Based on the R^2 values in decreasing order is Langmuir > Temkin > Sips > R–P > Freundlich. However, reports have shown that in the determination of the best-fit isotherm model, simply relying on the R^2 values alone is inadequate. This can be clearly seen from the error values in Table 2 where even though the Langmuir model gave the highest R^2 value, yet its overall error values were also the largest. The Freundlich model, often used for multilayer adsorption onto a heterogeneous surface, can also be ruled out as it gave the lowest R^2 value and second-highest errors. This is further confirmed from Fig. 4 when the experiment data and the simulated Langmuir and Freundlich models were compared. The same holds true for the R–P model, which appeared very similar and close to the Freundlich model.

In this study, the adsorption of CR onto WDFP seemed to indicate that of the five models employed, the Temkin model is the best fit model with good R^2 and lowest overall error values. The Temkin model assumes a uniform distribution of binding energies in an adsorption process with a linear decrease in the heat of adsorption as coverage on the surface by adsorbate increases. Its positive b_T value is indicative of an endothermic adsorption process. Table 2 also indicated that the Sips model, with $R^2 > 0.93$ and low errors, could also be a suitable model for the adsorption process. This model is a combination of the Langmuir and Freundlich models and is suitable for rough, heterogeneous adsorbent's surface. At low adsorbate concentration, it tends toward the Freundlich model, while at high adsorbate concentration, the Langmuir model is favored. The maximum adsorption capacity (q_{max}) of WDFP for the removal of BG based on the Sips model is 76.6 mg g^{-1}.

When compared to other fruit peels, WDFP showed higher maximum adsorption capacity (q_{max}) toward CR dye. Its adsorption ability toward CR is by far more superior to many reported natural adsorbents, as shown in Table 3, and even higher than that of cetyltrimethylammonium

Table 1
Equations of the isotherm models and error functions used in this study

Equations	
Isotherm models	Error functions
Langmuir	ARE
$\frac{C_e}{q_e}=\frac{1}{K_L q_{\max}}+\frac{C_e}{q_{\max}}$	$\frac{100}{n}\sum_{i=1}^{n}\left\|\frac{q_{e,\text{meas}}-q_{e,\text{calc}}}{q_{e,\text{meas}}}\right\|_i$
Freundlich	HYBRID
$\log q_e=\frac{1}{n}\log C_e+\log K_F$	$\frac{100}{n-p}\sum_{i=1}^{n}\left\|\frac{q_{e,\text{meas}}-q_{e,\text{calc}}}{q_{e,\text{meas}}}\right\|_i$
Temkin	EABS
$q_e=\left(\frac{RT}{b_T}\right)\ln K_T+\left(\frac{RT}{b_T}\right)\ln C_e$	$\sum_{i=1}^{n}\left\|q_{e,\text{meas}}-q_{e,\text{calc}}\right\|$
Redlich–Peterson	MSPD
$\ln\left(\frac{K_R C_e}{q_e}-1\right)=n\ln C_e+\ln a_R$	$100\sqrt{\frac{1}{n-p}\sum_{i=1}^{n}\left(\frac{q_{e,\text{meas}}-q_{e,\text{calc}}}{q_{e,\text{meas}}}\right)_i^2}$
Sips	χ^2
$\ln\left(\frac{q_e}{q_{\max}-q_e}\right)=\frac{1}{n}\ln C_e+\ln K_s$	$\sum_{i=1}^{n}\frac{\left(q_{e,\text{meas}}-q_{e,\text{calc}}\right)^2}{q_{e,\text{meas}}}$

bromide modified pumice [40] and N,N-dimethyl dehydroabietylamine oxide modified zeolite [41] with $q_{\max}$ of 27.3 and 69.9 mg g^{-1}, respectively. However, synthetic adsorbents showed much higher $q_{\max}$ [42–47]. Nevertheless, it must be emphasized that the WDFP used in this study was not subjected to any treatment, apart from being dried in an oven at 60°C. Therefore, as a low-cost natural adsorbent, WDFP is a potentially good candidate given its high $q_{\max}$ and its availability. Further, the possibility of enhancing its $q_{\max}$ through modification is viable, as shown by modification of adsorbents such as pumice [40], guava peel [48], eggshell membrane [49] and orange peel [50].

3.4. Adsorption kinetics of CR onto WDFP

The investigation into the adsorption kinetics on the removal of CR by WDFP was carried out using 100 mg L^{-1} dye concentration and the data obtained were then fitted using two commonly used models, namely the Lagergren pseudo-first-order [76] and the pseudo-second-order [77]. Although the linear plots of the two models in Figs. 5a and b both gave high $R^2 > 0.93$, error analyses of the two models using five different error functions showed that of the two models, the pseudo-second-order, with higher R^2 close to unity and overall smaller error values, as shown in Table 4, is a much better fit. This is further confirmed by the similar values of both the calculated adsorption capacity ($q_{e,\text{cal}}$) of pseudo-second-order kinetics and experiment adsorption capacity ($q_{e,\text{expt}}$). To further endorse the pseudo-second-order

Table 2
Results of adsorption of CR dye based on the five isotherm models used in this study

Model	Values	ARE	χ^2	HYBRID	EABS	MPSD
Langmuir		16.26	0.03	0.15	0.11	23.04
$q_{\max}$ (mmol g^{-1})	0.085					
K_L (L mmol^{-1})	0.010					
R^2	0.9642					
Freundlich		11.69	0.02	0.08	0.09	16.31
K_F (mmol g^{-1} (L mmol^{-1})$^{1/n}$)	0.005					
n	2.258					
R^2	0.8727					
Temkin		6.55	0.01	0.05	0.06	10.95
K_T (L mmol^{-1})	0.224					
b_T (kJ mol^{-1})	176.704					
R^2	0.9520					
Redlich–Peterson		10.96	0.02	0.08	0.08	15.25
K_R (L g^{-1})	0.004					
n	0.641					
a_R (L mmol^{-1})	0.442					
R^2	0.9132					
Sips		10.16	0.01	0.07	0.08	14.73
$q_{\max}$ (mmol g^{-1})	0.110					
K_S (L mmol^{-1})	0.025					
n	1.481					
R^2	0.9369					

kinetics, simulation of the data of two kinetics models were plotted and compared to the experimental data obtained. Fig. 5c clearly shows the close proximity of the pseudo-second-order to the experiment kinetics, whilst the Lagergren pseudo-first-order deviated from it. Hence, it can be concluded that the adsorption of CR onto WDFP followed the pseudo-second-order kinetics.

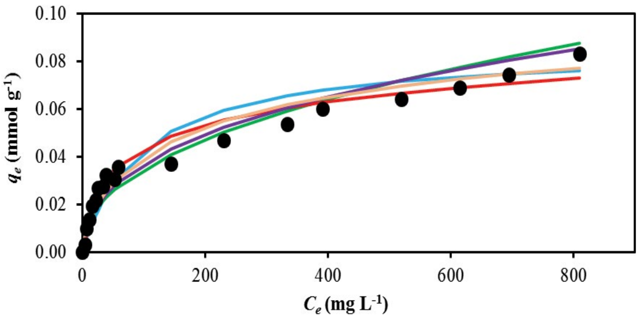

Fig. 4. Comparison of experiment isotherm data (●) with Langmuir (——), Freundlich (——), Temkin (——), R–P (——), and Sips (——) models.

In a solid-liquid such as an adsorbent-dye system, mass transport diffusion plays an important role. The diffusion mechanism usually involves several steps such as external mass transport of adsorbates from liquid phase across the boundary layer surrounding the adsorbent, adsorption onto the surface of an adsorbent, diffusion of adsorbates within the internal structure of the adsorbent through pore or surface. The diffusion mechanism in this study was evaluated using the Weber and Morris intraparticle diffusion model [78] and Fig. 6 showed that more than one step may be involved. The intercept on the y-axis at 0.0003 is very close to the origin, indicating that intraparticle diffusion could be the rate-controlling step.

3.5. Effect of pH on the adsorption of CR by WDFP

CR is sometimes used as an indicator as it changes color in both acidic and alkali conditions. The effect of pH was limited to the range of pH 4–12, since it was observed that

Table 3
Maximum adsorption capacity (q_{max}) of CR dye by various natural adsorbents

Adsorbent	q_{max} (mg g^{-1})	Reference
White dragon fruit peel	76.6 (Sips)	This work
	59.3 (Langmuir)	This work
Orange peel	22.4	[51]
Banana peel	44.4	[52]
Citrus limonum (lemon) peel	34.5	[53]
Raphanus sativus L. (Radish) peel	0.5	[54]
Pomelo peel	1.1	[55]
Watermelon rind	24.8	[56]
Guava peel	61.1	[48]
Tamarind fruit shell	10.5	[57]
Natural pumice	3.9	[40]
Peat	10.1	[58]
Red mud	4.5	[59]
Kaolin	5.4	[60]
Coir pith activated carbon	6.7	[61]
Myrtus communis activated carbon	19.2	[62]
Pomegranate activated carbon	10.0	[62]
Eucalyptus globulus sawdust	5.1	[63]
Pineapple (*Ananas comosus*) plant stem	12.0	[64]
Eichhornia crassipes roots	1.6	[65]
Ziziphus mauritiana (Jujube) seed	55.6	[66]
Cicer arietinum (Bengal gram) seed husk	41.7	[67]
Sugarcane bagasse	38.2	[68]
Apricot stone	32.9	[69]
Phoenix dactylifera seeds	61.7	[70]
Cattail root	38.8	[71]
Jute stick powder	35.7	[72]
Raw pine cone	32.7	[73]
Eggshell	69.5	[74]
Tea waste	32.3	[75]

under acidic condition (pH 2), the color of CR solution was altered and therefore results obtained would be invalid. As shown in Fig. 7, when compared to the untreated pH of CR at pH 5.5, WDFP did not show a large variation in its adsorption ability toward CR dye over the range of pH investigated. The maximum and minimum removals were observed at pH 12 and 10, respectively, with 6% increase and 15% reduction as compared to the untreated pH medium. At all other pH medium, only slight reduction (between 2%–7%) in the adsorption of CR was observed. This indicates that WDFP is relatively resilient to the changes in pH. Such a feature is attractive when applied to wastewater treatment since adsorbents that are not very much affected by pH could still maintain its adsorption ability and will thus be favored. Not all adsorbents showed resilience and are able to effectively removal CR under various pH. For example, Patel and Vashi [79] reported that Srujana seeds, maize powder, and chitosan showed drastic reduction (>40%) in their adsorption toward CR at high pH.

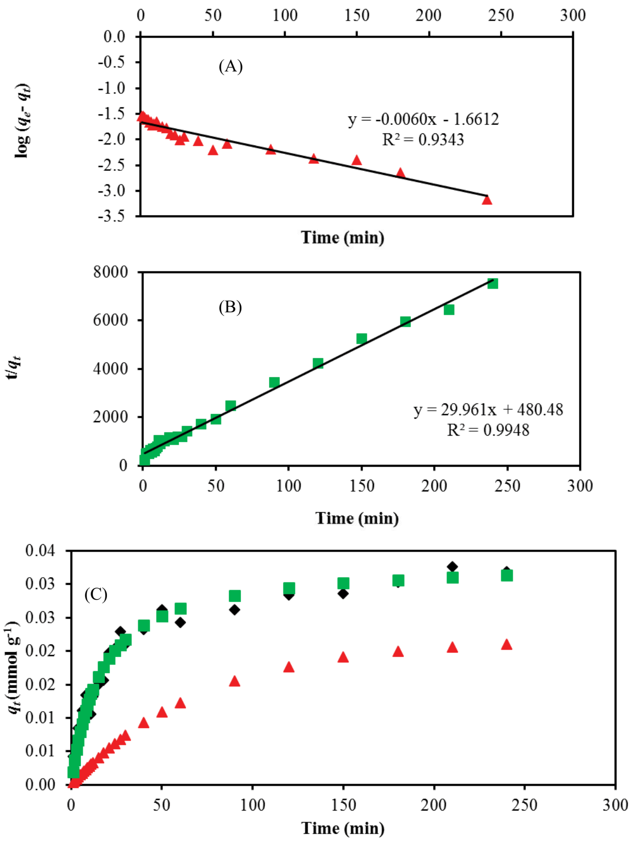

Fig. 5. (a) Linear plot of pseudo-first-order kinetics model, (b) linear plot of pseudo-second-order kinetics model, and (c) comparison of experiment kinetic data (●) with pseudo-first (▲) and pseudo-second (■) kinetics models.

3.6. Influence of salt concentration on the adsorption of CR by WDFP

Generally, depending on what is being disposed into the waterways, wastewater contains various electrolytes which may affect the adsorption of adsorbates onto adsorbents. Hence, an investigation on the effect of ionic strength is

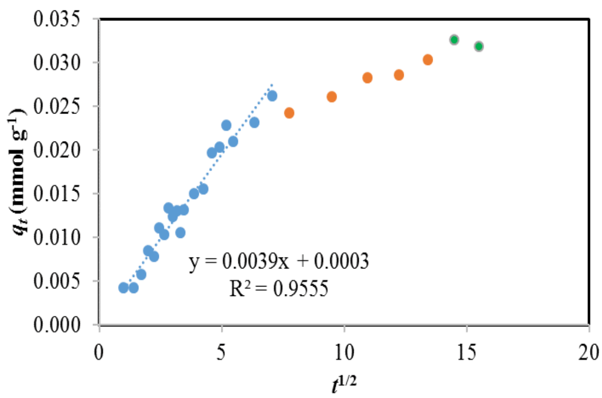

Fig. 6. Weber and Morris intraparticle diffusion of adsorption of CR onto WDFP.

Table 4
Results from the two kinetic models used for the adsorption of CR by WDFP

Model	Parameters	ARE	HYBRID	EABS	MPSD	χ^2
Lagergren pseudo-first-order		66.16	0.71	0.28	76.12	0.18
$\log(q_e - q_t) = \log(q_e) - \frac{k_1}{2.303}t$						
k_1 (min⁻¹)	0.014					
$q_{e,\mathrm{cal}}$ (mmol g⁻¹)	0.022					
Pseudo-second-order		9.51	0.02	0.03	16.16	0.01
$\frac{t}{q_e} = \frac{1}{k_2 q_e^2} + \frac{1}{q_e}t$						
k_2 (g mmol⁻¹ min⁻¹)	1.868					
$q_{e,\mathrm{cal}}$ (mmol g⁻¹)	0.032					
$q_{e,\mathrm{expt}}$ (mmol g⁻¹)	0.034					

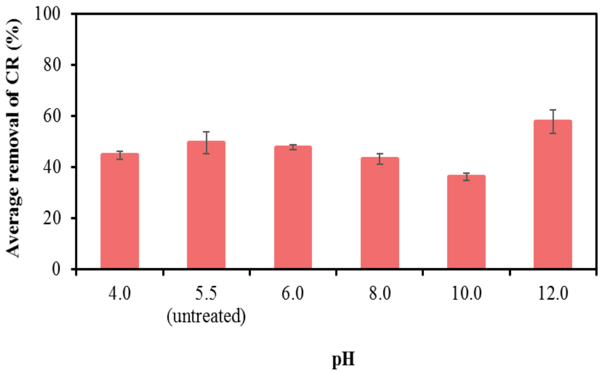

Fig. 7. Adsorption of CR onto WDFP in different pH medium.

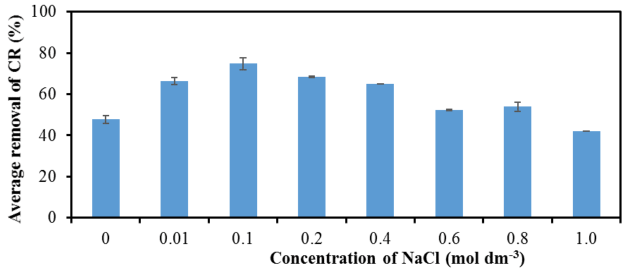

Fig. 8. Influence of adsorption of CR onto WDFP in different concentrations of NaCl.

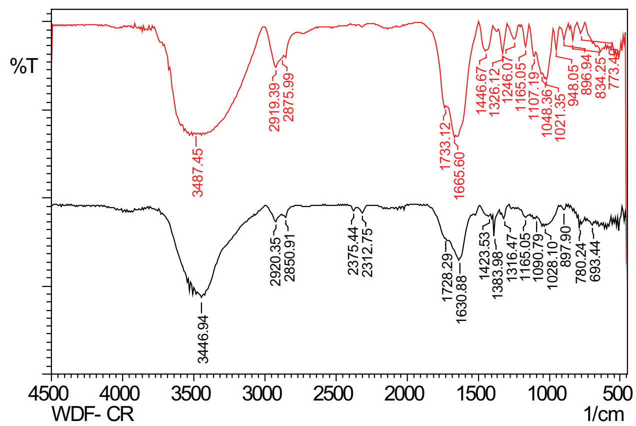

Fig. 9. FTIR spectra of WDFP before (red) and after adsorption (black) of CR dye.

one of the important factors in adsorption studies. Studies have shown that some adsorbents are greatly affected by the presence of ions in solution. Here, NaCl was chosen as the model salt and its effect on the adsorption of CR by WDFP was investigated over the range of 0 to 1 mol dm^{-3} salt concentration. Generally, compared to the absence of NaCl, WDFP showed a greater affinity toward CR dye in the presence of NaCl, with maximum dye removal of 75% at 0.1 mol dm^{-3} salt concentration (Fig. 8). At 1.0 mol dm^{-3} NaCl, a slight reduction of 6% was observed. Studies by both Han et al. [80] and Hu et al. [71] using rice husk and cattail root, respectively, were also in accordance to the above findings, attributing the increased in removal of CR to the reduction in repulsive forces between the surface functional groups on the adsorbent and the CR molecules as a result of screening effect of electrolytes, thereby leading to stronger electrostatic interactions between CR and the adsorbent. The ability for WDFP to not only maintain but enhanced its adsorption toward CR under various ionic strengths is an attractive feature in terms of utilizing it as a potential adsorbent in treating wastewater which usually has various electrolytes present.

3.7. Characterization of WDFP

3.7.1. Functional group determination by Fourier transform infrared spectroscopy

Fourier transform infrared spectroscopy (FTIR) spectrum of WDFP in Fig. 9 shows the presence of various functional groups peaks at 3,488 cm^{-1} (O–H, N–H), 2,876 cm^{-1} (CHO), 1,733 cm^{-1} (C=O), 1,666 cm^{-1} (C=O, C=C), 1,326 cm^{-1} (C–O, C–N). Upon CR adsorption, shifting of wavelengths to 3,447; 2,851; 1,728; 1,631 and 1,316 cm^{-1}, respectively were observed, indicating that these functional groups on the surface of WDFP could be involved in the adsorption of CR dye.

3.7.2. Scanning electron microscopy for surface morphology analysis

Scanning electron microscopy (SEM) images (Fig. 10) of the surface morphology of WDFP taken at 2,500× magnification prior to adsorption showed a highly uneven and rough surface with many undulating folds across the whole surface. This creates a bigger surface area for adsorption to take place and could be the reason why WDFP showed higher adsorption capacity towards CR dye than many reported natural adsorbents. There was a notable change in the surface morphology of WDFP after adsorption of CR dye. The rough surface of WDFP being now covered by CR dye molecules has become very much smoother.

3.7.3. Brunauer–Emmett–Teller of WDFP

Brunauer–Emmett–Teller (BET) (Model: Micromeritics ASAP™ 2020, USA) analysis of WDFP revealed its surface area, pore size, and pore volume to be 0.0925 m^2 g^{-1}, 0.00100 cm^3 g^{-1} and 43.24767 nm, respectively. Compared to many reported adsorbents such as activated carbon synthesized from *Pinus roxburghii* cone [81] and breadnut peel [82], WDFP has a much smaller surface area. Upon adsorption of CR dye, its surface area became negligible and could not be measured. This is most likely due to the dyes which have been adsorbed onto the surface of WDFP blocking all the adsorption sites.

3.7.4. Point of zero charge of WDFP

The determination of point of zero charges (pH$_{PZC}$) of an adsorbent is a useful characterization as it provides vital information on the electrical charge density of the adsorbent's surface when it is zero. This allows prediction on the surface

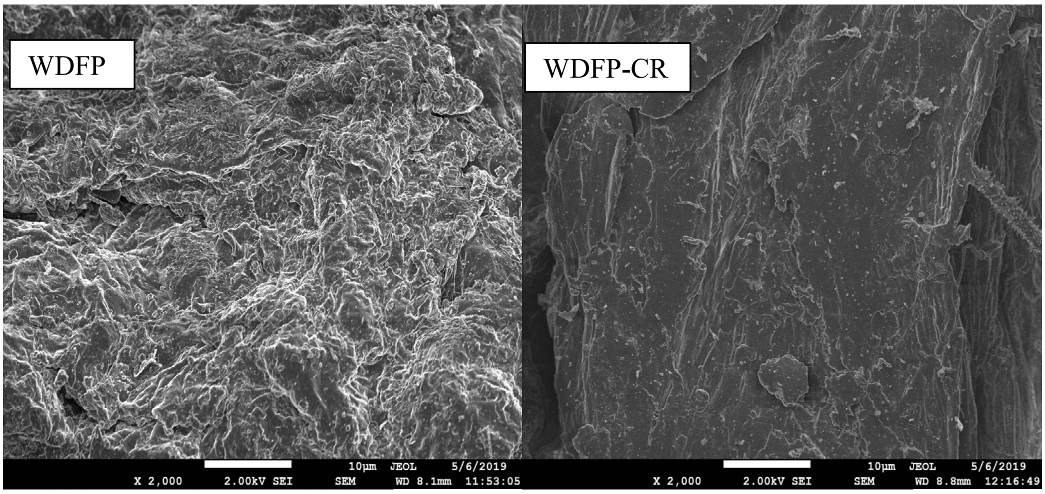

Fig. 10. SEM images of WDFP before and after adsorption of CR dye at 2,000× magnification.

charge when the adsorbent is in different pH medium. When pH > pH_{PZC}, functional groups on the surface of the adsorbent could undergo deprotonation, causing the surface to be predominantly negatively charged. The reverse holds true, that is when pH < pH_{PZC}, a predominantly positive charged surface could result due to protonation of the surface functional groups. This, in turn, will have an effect on the adsorption depending on whether the adsorbate is cationic or anionic in nature. In this study, pH_{PZC} of WDFP, carried out following the methods outlined by Lim et al. [83], was found to be at pH 5.02. A slight reduction of CR being adsorbed by WDFP was observed when pH > pH_{PZC} (up to pH 10) as shown in Fig. 7. This could be due to the negative surface charge on WDFP which hinders the adsorption of anionic CR dye as a result of repulsive electrostatic forces. However, the adsorption of CR onto WDFP may be more complex than it seemed.

3.8. Adsorption mechanism of CR onto WDFP

Different moieties may be involved in the adsorption mechanism of CR dye onto WDFP, giving rise to be a complex adsorption process (Fig. 11). The presence of negatively charged sulfonate (SO_3^-), amino (NH_2), naphthalene and biphenyl azo moieties provide possible interactions with functional groups present on the surface of WDFP. For example, the presence of SO_3^- on CR dye can result in attraction toward H atom on both O–H and N–H [84]. Apart from the expected H-bonding that can occur between adsorbent–adsorbate involving functional groups such as N–H, O–H, SO_3^-, COOH, Mazeau and Wyszomirski [85] has established that the biphenyl bond between the two symmetric aromatic parts of CR can undergo rotation which gives rise to substantial van der Waals attraction between the two aromatic moieties and the adsorbent's surface Xu et al. [44] also suggested the possibility of naphthalene in CR interacting with aromatic rings of adsorbent through stacking.

3.9. Regeneration and reusability of WDFP

In evaluating an adsorbent's efficiency as a potential adsorbent to be applied in wastewater treatment, the investigation of its ability to be regenerated and reused is of vital importance. From a practical point of view, an adsorbent that can be regenerated and reused will be more economical in terms of its cost as well as being more environmentally friendly. Hence, in this study, spent WDFP was tested for its ability to be regenerated and reused. Prior to carrying out regeneration studies, three desorbing solvents (1 mol dm^{-3} HCl, 1 mol dm^{-3} NaOH and water) were tested. Of these, NaOH and water did not desorb well (data not shown)

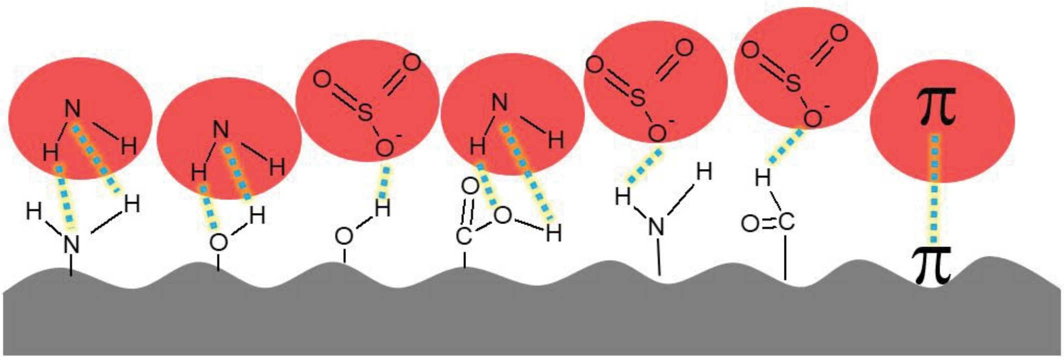

Fig. 11. Proposed adsorption mechanism of CR (●) onto WDFP (●).

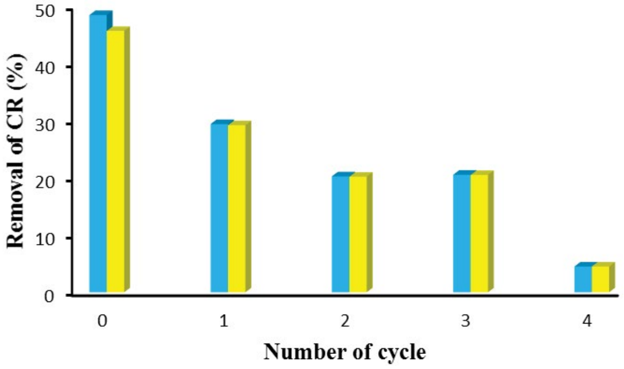

Fig. 12. Regeneration study of WDFP showing adsorption of CR (■) and desorption using 1 M HCl (■).

and hence, in this study 1 mol dm^{-3} HCl was selected as the desorbing solvent. Fig. 12 shows the results obtained for the regeneration study of WDFP. The CR loaded WDFP was successfully regenerated and reused for up to 4 consecutive cycles.

Not all adsorbents have been investigated for their reusability. For those that have been tested, there are some adsorbents such as Gum Arabic nanohydrogel [86] and arginine modified activated carbon [87] that still exhibit good adsorption capacity after several cycles, while other adsorbents required washing with base for them to be reused [6].

4. Conclusion

The peel of *Hylocereus undatus* (commonly known as white dragon fruit), which is inedible and regarded as waste and of no economic value, was successfully converted to potential and useful low-cost adsorbent for the removal of CR dye. This was demonstrated by its good adsorption capacity of 77 mg g^{-1} when compared to many reported natural adsorbents. Another attractive feature is that when placed in different pH medium, WDFP still has the ability to maintain good adsorption, showing relatively good resilience to changes in pH. Similarly, when placed in solutions of different ionic strengths, WDFP also performed well. Adsorption kinetics fitted closely to the pseudo-second-order model and intraparticle diffusion could be the rate-controlling step. The above results coupled with it being an abundant low-cost agriculture waste, indicate that WDFP could well be considered a possible candidate in real-life wastewater treatment application.

Acknowledgment

The authors wish to express their sincere thanks to the Government of Brunei Darussalam, the Universiti Brunei Darussalam (UBD) for their continuous support and also to the Physical and Geological Sciences Program @ UBD for the use of SEM instrument.

References

[1] G. Sharma, A. Kumar, S. Sharma, A.H. Al-Muhtaseb, Mu. Naushad, A.A. Ghfar, T. Ahamad, F.J. Stadler, Fabrication and characterization of novel Fe^0@Guar gum-crosslinked-soya lecithin nanocomposite hydrogel for photocatalytic degradation of methyl violet dye, Sep. Purif. Technol., 211 (2019) 895–908.
[2] M.A. Rauf, S. Salman Ashraf, Survey of recent trends in biochemically assisted degradation of dyes, Chem. Eng. J., 209 (2012) 520–530.
[3] M.T. Yagub, T.K. Sen, S. Afroze, H.M. Ang, Dye and its removal from aqueous solution by adsorption: a review, Adv. Colloid Interface Sci., 209 (2014) 172–184.
[4] N.B. Singh, G. Nagpal, S. Agrawal, Rachna, Water purification by using adsorbents: a review, Environ. Technol. Innovation, 11 (2018) 187–240.
[5] M.R.R. Kooh, M.K. Dahri, L.B.L. Lim, L.H. Lim, Batch adsorption studies on the removal of Acid Blue 25 from aqueous solution using azolla pinnata and soya bean waste, Arabian J. Sci. Eng., 41 (2016) 2453–2464.
[6] M.K. Dahri, L.B.L. Lim, C.C. Mei, Cempedak durian as a potential biosorbent for the removal of Brilliant Green dye from aqueous solution: equilibrium, thermodynamics and kinetics studies, Environ. Monit. Assess., 187 (2015) 546.
[7] K.S. Bharathi, S.T. Ramesh, Removal of dyes using agricultural waste as low-cost adsorbents: a review, Appl. Water Sci., 3 (2013) 773–790.
[8] J. Mo, Q. Yang, N. Zhang, W. Zhang, Y. Zheng, Z. Zhang, A review on agro-industrial waste (AIW) derived adsorbents for water and wastewater treatment, J. Environ. Manage., 227 (2018) 395–405.
[9] L.R. Bonetto, F. Ferrarini, C. de Marco, J.S. Crespo, R. Guégan, M. Giovanela, Removal of methyl violet 2B dye from aqueous solution using a magnetic composite as an adsorbent, J. Water Process Eng., 6 (2015) 11–20.
[10] Mu. Naushad, S. Vasudevan, G. Sharma, A. Kumar, Z.A. ALOthman, Adsorption kinetics, isotherms, and thermodynamic studies for Hg^{2+} adsorption from aqueous medium using alizarin red-S-loaded amberlite IRA-400 resin, Desal. Wat. Treat., 57 (2016) 18551–18559.
[11] L.B.L. Lim, N. Priyantha, T. Zehra, C.W. Then, C.M. Chan, Adsorption of crystal violet dye from aqueous solution onto chemically treated *Artocarpus odoratissimus* skin: equilibrium, thermodynamics, and kinetics studies, Desal. Water Treat., 57 (2016) 10246–10260.
[12] H.I. Chieng, L.B.L. Lim, N. Priyantha, Enhancement of crystal violet dye adsorption on artocarpus camansi peel through sodium hydroxide treatment, Desal. Wat. Treat., 58 (2017) 320–331.
[13] G. Sharma. A. Kumar, K. Devi, S. Sharma, Mu. Naushad, A.A. Ghfar, Guar gum-crosslinked-Soya lecithin nanohydrogel sheets as effective adsorbent for the removal of thiophanate methyl fungicide, Int. J. Biol. Macromol., 114 (2018) 295–305.
[14] G. Sharma, B. Thakur, Mu. Naushad, A. Kumar, F.J. Stadler, S.M. Alfadul, G.T. Mola, Applications of nanocomposite hydrogels for biomedical engineering and environmental protection, Environ. Chem. Lett., 16 (2018) 113–146.
[15] G. Sharma, S. Sharma, A. Kumar, A.H. Al-Muhtaseb, Mu. Naushad, A.A. Ghfar, G.T. Mola, F.J. Stadler, Guar gum and its composites as potential materials for diverse applications: a review, Carbohydr. Polym., 199 (2018) 534–545.
[16] L.B.L. Lim, N. Priyantha, Y. Lu, N.A.H. Mohamad Zaidi, Effective removal of methyl violet dye using pomelo leaves as a new low-cost adsorbent, Desal. Wat. Treat., 110 (2018) 264–274.
[17] W.S. Choo, W.K. Yong, Antioxidant properties of two species of *Hylocereus* fruits, Plagia Res. Lib., 2 (2011) 418–425.
[18] B. Jamilah, C.E. Shu, M. Kharidah, M.A. Dzulkifly, A. Noranizan, Physico-chemical characteristics of red pitaya (*Hylocereus polyrhizus*) peel, Int. Food Res. J., 18 (2011) 279–286.
[19] S. Priatni, A. Pradita, Stability study of betacyanin extract from red dragon fruit (*Hylocereus polyrhizus*) peels, Procedia Chem., 16 (2015) 438–444.
[20] K.K. Woo, F.H. Ngou, W.K. Soong, P.Y. Tang, Stability of betalain pigment from red dragon fruit (*Hylocereus polyrhizus*), Am. J. Food Technol., 6 (2011) 140–148.
[21] H. Luo, Y. Cai, Z. Peng, T. Liu, S. Yang, Chemical composition and in vitro evaluation of the cytotoxic and antioxidant activities of supercritical carbon dioxide extracts of pitaya (dragon fruit) peel, Chem. Cent. J., 8 (2014) 1–7.

[22] A.H. Jawad, A.M. Kadhum, Y.S. Ngoh, Applicability of dragon fruit (*Hylocereus polyrhizus*) peels as low-cost biosorbent for adsorption of methylene blue from aqueous solution: kinetics, equilibrium and thermodynamics studies, Desal. Wat. Treat., 109 (2018) 231–240.

[23] N. Priyantha, L.B.L. Lim, M.K. Dahri, Dragon fruit skin as a potential biosorbent for the removal of methylene blue dye from aqueous solution, Int. Food Res. J., 22 (2015) 2141–2148.

[24] R. Mallampati, L. Xuanjun, A. Adin, S. Valiyaveettil, Fruit peels as efficient renewable adsorbents for removal of dissolved heavy metals and dyes from water, ACS Sustainable Chem. Eng., 3 (2015) 1117–1124.

[25] A.M. Tanasal, N. La Nafie, P. Taba, Biosorption of Cd(II) ion by dragon fruit peel (*Hylocereus polyrhizus*), J. Akta Kim. Indones. (Indonesia Chim. Acta), 8 (2015) 18–30.

[26] N. Priyantha, L.B.L. Lim, M.K. Dahri, D.T.B. Tennakoon, Dragon fruit skin as a potential low-cost biosorbent for the removal of manganese(II) ions, J. Appl. Sci. Environ. Sanit., 8 (2013) 179–188.

[27] Z.Z. Abidin, H. Zahra, M.A. Shavandi, M.H. Shah Ismail, F.-R. Ahmadun, Methylene Blue removal from aqueous solution by *Hylocereus undatus* (dragon fruit) foliage, Appl. Mech. Mater., 625 (2014) 864–869.

[28] Z. Haddadian, M.A. Shavandi, Z. Abidin, A. Fakhru'l-Razi, M. Halim, S. Ismail, Removal methyl orange from aqueous solutions using dragon fruit (*Hylocereusundatus*) foliage, Chem. Sci. Trans., 2 (2013) 900–910.

[29] D.P. Steensma, "Congo" red: out of Africa?, Arch. Pathol. Lab. Med., 125 (2001) 250–252.

[30] O. Hörstensmeyer, Tödlicher Zwischenfall nach intravenöser Injektion von Kongorot, DMW - Dtsch. Medizinische Wochenschrift, 89 (1964) 1845–1848.

[31] C. Schilliger-Musset, Inclusion of Substances of Very High Concern in the Candidate List for Eventual Inclusion in Annex XIV, European Chemicals Agency, ED/121/2013, 2013, pp. 1–5.

[32] E.I. Yakupova, L.G. Bobyleva, I.M. Vikhlyantsev, A.G. Bobylev, Congo red and amyloids: history and relationship, Biosci. Rep., BSR20181415, 39 (2019) 1–22.

[33] N. Asses, L. Ayed, N. Hkiri, M. Hamdi, Congo red decolorization and detoxification by *Aspergillus niger*: removal mechanisms and dye degradation pathway, BioMed Res. Int., 7 (2018) 1–9.

[34] D.I. Macht, W.C. Harden, M.L. Grumbein, Toxicological studies on Congo red, J. Am. Pharm. Assoc., 28 (1939) 495–499.

[35] I. Langmuir, The adsorption of gases on plane surfaces of glass, mica and platinum, J. Am. Chem. Soc., 40 (1918) 1361–1403.

[36] H. Freundlich, Over the adsorption in the solution, J. Phys. Chem., 57 (1906) 385–470.

[37] M.J. Temkin, V. Pyzhev, Kinetics of ammonia synthesis on promoted iron catalysts, Acta Phys., 12 (1940) 217.

[38] O. Redlich, D.L. Peterson, A useful adsorption isotherm, J. Phys. Chem., 63 (1959) 1024.

[39] R. Sips, On the structure of a catalyst surface, J. Chem. Phys., 16 (1948) 490–495.

[40] H. Shayesteh, A. Rahbar-Kelishami, R. Norouzbeigi, Evaluation of natural and cationic surfactant modified pumice for Congo red removal in batch mode: kinetic, equilibrium, and thermodynamic studies, J. Mol. Liq., 221 (2016) 1–11.

[41] S. Liu, Y. Ding, P. Li, K. Diao, X. Tan, F. Lei, Y. Zhan, Q. Li, B. Huang, Z. Huang, Adsorption of the anionic dye Congo red from aqueous solution onto natural zeolites modified with N,N-dimethyl dehydroabietylamine oxide, Chem. Eng. J., 248 (2014) 135–144.

[42] S. Ghorai, A.K. Sarkar, A.B. Panda, S. Pal, Effective removal of Congo red dye from aqueous solution using modified xanthan gum/silica hybrid nanocomposite as adsorbent, Bioresour. Technol., 144 (2013) 485–491.

[43] M. Bhaumik, R. McCrindle, A. Maity, Efficient removal of Congo red from aqueous solutions by adsorption onto interconnected polypyrrole–polyaniline nanofibres, Chem. Eng. J., 228 (2013) 506–515.

[44] J. Xu, D. Xu, B. Zhu, B. Cheng, C. Jiang, Adsorptive removal of an anionic dye Congo red by flower-like hierarchical magnesium oxide (MgO)-graphene oxide composite microspheres, Appl. Surf. Sci., 435 (2018) 1136–1142.

[45] A. Afkhami, R. Moosavi, Adsorptive removal of Congo red, a carcinogenic textile dye, from aqueous solutions by maghemite nanoparticles, J. Hazard. Mater., 174 (2010) 398–403.

[46] J. Liu, N. Wang, H. Zhang, J. Baeyens, Adsorption of Congo red dye on $Fe_xCo_3–xO_4$ nanoparticles, J. Environ. Manage., 238 (2019) 473–483.

[47] Y. Bao, M. Qin, Y. Yu, L. Zhang, H. Wu, Facile fabrication of porous $NiCo_2O_4$ nanosheets with high adsorption performance toward Congo red, J. Phys. Chem. Solids, 124 (2019) 289–295.

[48] P. Singh, P. Raizada, D. Pathania, G. Sharma, P. Sharma, Microwave induced KOH activation of guava peel carbon as an adsorbent for Congo red dye removal from aqueous phase, Ind. J. Chem. Technol., 20 (2013) 305–311.

[49] S. Parvin, B.K. Biswas, M.A. Rahman, M.H. Rahman, M.S. Anik, M.R. Uddin, Study on adsorption of Congo red onto chemically modified egg shell membrane, Chemosphere, 236 (2019) 124326.

[50] V.S. Munagapati, D.-S. Kim, Adsorption of anionic azo dye Congo red from aqueous solution by cationic modified orange peel powder, J. Mol. Liq., 220 (2016) 540–548.

[51] C. Namasivayam, N. Muniasamy, K. Gayatri, M. Rani, K. Ranganathan, Removal of dyes from aqueous solutions by cellulosic waste orange peel, Bioresour. Technol., 57 (1996) 37–43.

[52] Sumanjit, S. Rani, R.K. Mahajan, Kinetic and equilibrium studies of adsorption of dye Congo red from aqueous solutions on bagasse charcoal and banana peels, J. Surf. Sci. Technol., 28 (2012) 133–147.

[53] A. Bhatnagar, E. Kumar, A.K. Minocha, B.-H. Jeon, H. Song, Y.-C. Seo, Removal of anionic dyes from water using *Citrus limonum* (lemon) peel: equilibrium studies and kinetic modeling, Sep. Sci. Technol., 44 (2009) 316–334.

[54] A. Abbas, S. Murtaza, M. Munir, T. Zahid, N. Abbas, A. Mushtaq, Removal of Congo red from aqueous solutions with *Raphanus sativus* peels and activated carbon: a comparative study, Am.-Eurasian J. Agric. Environ. Sci., 10 (2011) 802–809.

[55] M. Jayarajan, R. Arunachala, G. Annadurai, Use of low cost nano-porous materials of pomelo fruit peel wastes in removal of textile dye, Res. J. Environ. Sci., 5 (2011) 434–443.

[56] M.B. Sani, Comparative isotherms studies on adsorptive removal of Congo red from wastewater by watermelon rinds and neem-tree leaves, Open J. Phys. Chem., 4 (2014) 139–146.

[57] S. Reddy, Removal of direct dye from aqueous solutions with an adsorbent made from tamarind fruit shell, an agricultural solid waste, J. Sci. Ind. Res., 65 (2006) 443–446.

[58] T. Zehra, N. Priyantha, L.B.L. Lim, E. Iqbal, Sorption characteristics of peat of Brunei Darussalam V: removal of Congo red dye from aqueous solution by peat, Desal. Wat. Treat., 54 (2015) 2592–2600.

[59] C. Namasivayam, D.J.S.E. Arasi, Removal of Congo red from wastewater by adsorption onto waste red mud, Chemosphere, 34 (1997) 401–417.

[60] V. Vimonses, S. Lei, B. Jin, C.W.K. Chow, C. Saint, Kinetic study and equilibrium isotherm analysis of Congo red adsorption by clay materials, Chem. Eng. J., 148, (2009) 354–364.

[61] C. Namasivayam, D. Kavitha, Removal of Congo red from water by adsorption onto activated carbon prepared from coir pith, an agricultural solid waste, Dyes Pigm., 54 (2002) 47–58.

[62] M. Ghaedi, H. Tavallali, M. Sharifi, S.N. Kokhdan, A. Asghari, Preparation of low cost activated carbon from *Myrtus communis* and pomegranate and their efficient application for removal of Congo red from aqueous solution, Spectrochim. Acta, Part A, 86 (2012) 107–114.

[63] V.S. Mane, P.V. Vijay Babu, Kinetic and equilibrium studies on the removal of Congo red from aqueous solution using Eucalyptus wood (*Eucalyptus globulus*) saw dust, J. Taiwan Inst. Chem. Eng., 44 (2013) 81–88.

[64] S.-L. Chan, Y.P. Tan, A.H. Abdullah, S.-T. Ong, Equilibrium, kinetic and thermodynamic studies of a new potential biosorbent for the removal of Basic Blue 3 and Congo red dyes: pineapple (*Ananas comosus*) plant stem, J. Taiwan Inst. Chem. Eng., 61 (2016) 306–315.

[65] W.C. Wanyonyi, J.M. Onyari, P.M. Shiundu, Adsorption of Congo red dye from aqueous solutions using roots of *Eichhornia crassipes*: kinetic and equilibrium studies, Energy Procedia, 50 (2014) 862–869.
[66] M.C. Somasekhara Reddy, L. Sivaramakrishna, A. Varada Reddy, The use of an agricultural waste material, Jujuba seeds for the removal of anionic dye (Congo red) from aqueous medium, J. Hazard. Mater., 203–204 (2012) 118–127.
[67] M.C. Somasekhara Reddy, V. Nirmala, C. Ashwini, Bengal gram seed husk as an adsorbent for the removal of dye from aqueous solutions – batch studies, Arabian J. Chem., 10 (2017) S2554–S2566.
[68] Z. Zhang, L. Moghaddam, I.M. O'Hara, W.O.S. Doherty, Congo red adsorption by ball-milled sugarcane bagasse, Chem. Eng. J., 178 (2011) 122–128.
[69] M. Abbas, M. Trari, Kinetic, equilibrium and thermodynamic study on the removal of Congo red from aqueous solutions by adsorption onto apricot stone, Process Saf. Environ. Prot., 98 (2015) 424–436.
[70] D. Pathania, A. Sharma, Z.-M. Siddiqi, Removal of Congo red dye from aqueous system using *Phoenix dactylifera* seeds, J. Mol. Liq., 219 (2016) 359–367.
[71] Z. Hu, H. Chen, F. Ji, S. Yuan, Removal of Congo red from aqueous solution by cattail root, J. Hazard. Mater., 173 (2010) 292–297.
[72] G.C. Panda, S.K. Das, A.K. Guha, Jute stick powder as a potential biomass for the removal of Congo red and rhodamine B from their aqueous solution, J. Hazard. Mater., 164 (2009) 374–379.
[73] S. Dawood, T.K. Sen, Removal of anionic dye Congo red from aqueous solution by raw pine and acid-treated pine cone powder as adsorbent: equilibrium, thermodynamic, kinetics, mechanism and process design, Water Res., 46 (2012) 1933–1946.
[74] P. Das Saha, S. Chowdhury, M. Mondal, K. Sinha, Biosorption of Direct Red 28 (Congo red) from aqueous solutions by eggshells: batch and column studies, Sep. Sci. Technol., 47 (2012) 112–123.
[75] M. Foroughi-Dahr, H. Abolghasemi, M. Esmaili, A. Shojamoradi, H. Fatoorehchi, Adsorption characteristics of Congo red from aqueous solution onto tea waste, Chem. Eng. Commun., 202 (2015) 181–193.
[76] S. Lagergren, About the theory of so-called adsorption of soluble substances, K. Sven. Vetenskapsakad. Handl., 24 (1898) 1–39.
[77] Y.S. Ho, G. McKay, Sorption of dye from aqueous solution by peat, Chem. Eng. J., 70 (1998) 115–124.
[78] W. Weber, J. Morris, Kinetics of adsorption on carbon from solution, J. Sanit. Eng. Div., 89 (1963) 31–60.
[79] H. Patel, R.T. Vashi, Removal of Congo red dye from its aqueous solution using natural coagulants, J. Saudi Chem. Soc., 16 (2012) 131–136.
[80] R. Han, D. Ding, Y. Xu, W. Zou, Y. Wang, Y. Li, L. Zou, Use of rice husk for the adsorption of Congo red from aqueous solution in column mode, Bioresour. Technol., 99 (2008) 2938–2946.
[81] G. Sharma, S. Sharma, A. Kumar, Mu. Naushad, B. Du, T. Ahamad, A.A. Ghfar, A. Alqadami, F.J. Stadler, Honeycomb structured activated carbon synthesized from *Pinus roxburghii* cone as effective bioadsorbent for toxic malachite green dye, J. Water Process Eng., 32 (2019) 100931.
[82] L.B.L. Lim, N. Priyantha, D.T.B. Tennakoon, H.I. Chieng, M.K. Dahri, M. Suklueng, Breadnut peel as a highly effective low-cost biosorbent for methylene blue: equilibrium, thermodynamic and kinetic studies, Arabian J. Chem., 10 (2017) S3216–S3228.
[83] L.B.L. Lim, N. Priyantha, N.H. Mohd Mansor, *Artocarpus altilis* (breadfruit) skin as a potential low-cost biosorbent for the removal of crystal violet dye: equilibrium, thermodynamics and kinetics studies, Environ. Earth Sci., 73 (2015) 3239–3247.
[84] K. Sharma, V. Kumar, B.S. Kaith, V. Kumar, S. Som, S. Kalia, H.C. Swart, Synthesis, characterization and water retention study of biodegradable gum ghatti-poly(acrylic acid–aniline) hydrogels, Polym. Degrad. Stab., 111 (2015) 20–31.
[85] K. Mazeau, M. Wyszomirski, Modelling of Congo red adsorption on the hydrophobic surface of cellulose using molecular dynamics, Cellulose, 19 (2012) 1495–1506.
[86] G. Sharma, A. Kumar, Mu. Naushad, A. García-Peñas, A.H. Al-Muhtaseb, A.A. Ghfar, V. Sharma, T. Ahamad, F.J. Stadler, Fabrication and characterization of Gum arabic-cl-poly(acrylamide) nanohydrogel for effective adsorption of crystal violet dye, Carbohydr. Polym., 202 (2018) 444–453.
[87] M. Naushad, A.A. Alqadami, Z.A. AlOthman, I.H. Alsohaimi, M.S. Algamdi, A.M. Aldawsari, Adsorption kinetics, isotherm and reusability studies for the removal of cationic dye from aqueous medium using arginine modified activated carbon, J. Mol. Liq., 293 (2019) 111442.